New Journal of Physics
The open access journal at the forefront of physics

Deutsche Physikalische Gesellschaft DPG IOP Institute of Physics

PAPER • OPEN ACCESS

Tissue evolution: mechanical interplay of adhesion, pressure, and heterogeneity

To cite this article: Tobias Büscher *et al* 2020 *New J. Phys.* **22** 033048

View the article online for updates and enhancements.

You may also like

- NRPB Chilton Seminar: Professor Bryn Bridges—`Genetic Effects of Radiation: Are the Paradigms Changing?' (Chilton, November 2001)
- Cellular reprogramming dynamics follow a simple 1D reaction coordinate
Sai Teja Pusuluri, Alex H Lang, Pankaj Mehta et al.
- Modeling the impact of granular embedding media, and pulling versus pushing cells on growing cell clones
Dirk Drasdo and Stefan Hoehme

This content was downloaded from IP address 103.244.5.250 on 02/10/2026 at 08:35

New Journal of Physics
The open access journal at the forefront of physics

Deutsche Physikalische Gesellschaft DPG
IOP Institute of Physics

Published in partnership with: Deutsche Physikalische Gesellschaft and the Institute of Physics



OPEN ACCESS

RECEIVED
15 October 2019

REVISED
8 January 2020

ACCEPTED FOR PUBLICATION
10 February 2020

PUBLISHED
25 March 2020

Original content from this work may be used under the terms of the Creative Commons Attribution 4.0 licence.

Any further distribution of this work must maintain attribution to the author(s) and the title of the work, journal citation and DOI.



PAPER

Tissue evolution: mechanical interplay of adhesion, pressure, and heterogeneity

Tobias Büscher[1], **Nirmalendu Ganai**[1,2], **Gerhard Gompper**[1] and **Jens Elgeti**[1]

[1] Theoretical Soft Matter and Biophysics, Institute of Complex Systems and Institute for Advanced Simulation, Forschungszentrum Jülich, D-52425, Jülich, Germany
[2] Department of Physics, Nabadwip Vidyasagar College, Nabadwip, Nadia 741302, India

E-mail: j.elgeti@fz-juelich.de

Keywords: tumor heterogeneity, tumorigenesis, tissue competition, homeostatic pressure, evolution

Supplementary material for this article is available online

Abstract

The evolution of various competing cell types in tissues, and the resulting persistent tissue population, is studied numerically and analytically in a particle-based model of active tissues. Mutations change the properties of cells in various ways, including their mechanical properties. Each mutation results in an advantage or disadvantage to grow in the competition between different cell types. While changes in signaling processes and biochemistry play an important role, we focus on changes in the mechanical properties by studying the result of variation of growth force and adhesive cross-interactions between cell types. For independent mutations of growth force and adhesion strength, the tissue evolves towards cell types with high growth force and low internal adhesion strength, as both increase the homeostatic pressure. Motivated by biological evidence, we postulate a coupling between both parameters, such that an increased growth force comes at the cost of a higher internal adhesion strength or vice versa. This tradeoff controls the evolution of the tissue, ranging from unidirectional evolution to very heterogeneous and dynamic populations. The special case of two competing cell types reveals three distinct parameter regimes: two in which one cell type outcompetes the other, and one in which both cell types coexist in a highly mixed state. Interestingly, a single mutated cell alone suffices to reach the mixed state, while a finite mutation rate affects the results only weakly. Finally, the coupling between changes in growth force and adhesion strength reveals a mechanical explanation for the evolution towards intra-tumor heterogeneity, in which multiple species coexist even under a constant evolutionary pressure.

1. Introduction

Mutations change the cell fitness and thus its chance to survive and proliferate [1]. Advantageous mutations are more likely to persist due to natural selection, which drives the evolution of a tissue towards fitter cells [2]. Cancer represents an example of evolution on a short time scale [3]. Furthermore, cancer is a multistep process, i.e. several mutations are needed for a tumor in order to develop and become malignant [4]. Hence, tumorigenesis might be expected to happen in a serial manner, i.e. a cell acquiring a 'beneficial' mutation and taking over the whole tissue. After some time, a daughter cell acquires another mutation and again takes over. Interestingly, however, tumors do not consist of a single cell type, but instead several subpopulations coexist within the same tumor. This is called intra-tumor heterogeneity [5].

Each mutation changes certain biochemical properties of a cell. This ranges from misfunction in the error correction machinery during DNA replication and disruptions in signaling pathways to epigenetic changes in the expression level of certain proteins [1, 6, 7]. All these changes can also affect the mechanical properties of the mutated cell, e.g. mutated cells which express less adhesion proteins might be able to detach from the primary tumor more easily [8], a necessary step for the formation of metastases. However, the metastatic process seems to

© 2020 The Author(s). Published by IOP Publishing Ltd on behalf of the Institute of Physics and Deutsche Physikalische Gesellschaft

be more complex, as adhesion proteins such as E-cadherin are still found in metastatic cells, while a recent study points out that E-cadherin might even be necessary in order to form metastases [9]. On the other hand, mechanics feeds back onto growth in several ways, e.g. increased apoptosis rate due to mechanical stresses [10, 11] or dependence of the growth of tissue spheroids on the properties of the surrounding medium [12–14].

It is the mechanical contribution to tissue development that we want to focus on in this work. For mechanically regulated growth, homeostatic pressure plays an important role [15]. In the homeostatic state, when apoptosis and division balance each other, a tissue exerts a certain pressure onto its surrounding, the homeostatic pressure P_{H}. The tissue is able to grow as long as the external pressure P is smaller than P_{H}. For the competition between different tissues for space, it has been suggested that the tissue with the higher homeostatic pressure grows at the expense of the weaker tissue. Several theoretical studies employ this concept in order to describe interface propagation between two competing tissues [16–18]. A metastasis would need to reach a critical size, below which the additional Laplace pressure due to surface tension would cause the metastasis to shrink and disappear [15]. However, reduced adhesion between tissues, which increases surface tension, leads to an enhanced growth rate at the interface between them, stabilizing coexistence even for differing homeostatic pressures [19].

The evolutionary aspect of tumor development has been studied extensively under the viewpoint of resistance to chemotherapy [20]. Heterogeneities can contribute to the evolution of resistance to certain drug treatments not only in the cancer cell phenotypes but also in the tumor microenvironment [21]. A main research focus is the design of treatment strategies which take already existing resistances and the development of new resistances into account [21, 22]. Resistance may come at the cost of a fitness disadvantage in the absence of therapy. This lead to the proposal of adaptive therapy, in which a stable, non-resistant population is maintained by low-dose treatment, which then suppresses proliferation of resistant phenotypes [23, 24].

A related system of clusters and swarms of growing and dividing cells with a significant mutation rate are bacterial colonies and biofilms [25, 26]. These are interesting model systems, because they can easily be cultured and studied *in vitro* experimentally. For example, the gene expression in various cell types can be detected by fluorescent fusion proteins [27]. Therefore, detailed studies of bacterial colonies can help to understand how properties of microscopic cellular components determine macroscopic, multicellular biological function.

In this work, we study the influence of mutations that change the mechanical properties of cells on the competition dynamics, especially the interplay between changes in the adhesive properties and the strength with which a cell pushes onto its surrounding. Particularly interesting is the case where loss of adhesion comes at the cost of lower growth strength. This is motivated by the observed down-regulation of E-cadherin, an adhesion protein in epithelia, in many types of cancer [28]. Interestingly, E-cadherin is also involved in signaling processes connected to cell growth [29]. We find that in this case several cell types with different mechanical properties can coexist and that the cell type with the highest homeostatic pressure does not necessarily dominate the competition.

2. Simulation model

Several models have been developed previously in order to study tissue growth [30], in combination with different simulation techniques, including vertex [31, 32] and particle-based [33, 34] models as well as Cellular Potts models [35, 36]. We employ the two particle growth (2PG) model of [19, 37, 38]. A cell is described by two particles which repel each other via a growth force

$$F_{ij}^{\mathrm{G}} = \frac{G}{(r_{ij} + r_0)^2}\hat{\boldsymbol{r}}_{ij}, \tag{1}$$

with strength G, unit vector $\hat{\boldsymbol{r}}_{ij}$, distance r_{ij} between the two particles and a constant r_0. Different cells interact via a soft repulsive force F_{ij}^{V} on short distances, maintaining an excluded volume, and a constant attractive force F_{ij}^{A} on intermediate distances, modeling cell–cell adhesion, with

$$\left.\begin{aligned} F_{ij}^{\mathrm{V}} &= f_0\left(\frac{R_{\mathrm{PP}}^5}{r_{ij}^5} - 1\right)\hat{\boldsymbol{r}}_{ij} \\ F_{ij}^{\mathrm{A}} &= -f_1\hat{\boldsymbol{r}}_{ij} \end{aligned}\right\} \text{for } r_{ij} < R_{\mathrm{PP}}, \tag{2}$$

with exclusion coefficient f_0, adhesion strength coefficient f_1, and cut-off length R_{PP}. A cell divides when the distance between its two particles reaches a size threshold r_{ct}. A new particle is then placed close (randomly within a short distance r_{d}) to each of the two particles of the divided cell. Each of these pairs then constitutes a new cell. Apoptosis is modeled by removing cells randomly at a constant rate k_{a}.

In real cells, the cell cycle and the cell division process are correlated with mechanical forces, but not fully determined by it [39]. Hence, in order to study the influence of the details of the division mechanism, we also

employ a division mechanism, where cells divide with a finite rate k_{div} after reaching a smaller size treshold $r'_{\mathrm{ct}} < r_{\mathrm{ct}}$. The growth force equation (1) is set to zero when the distance between the two particles exceeds r_{ct}. This mechanism leads to a broader distribution of cell sizes at division and an additional source of randomness [40, 41]. Unless otherwise mentioned, the sharp threshold division mechanism is employed.

We employ a dissipative particle dynamics-type thermostat, with an effective temperature T, to account for energy dissipation and random fluctuations. We choose the value of T such that cells can escape local minima, but other thermal effects are negligible. Note that all parameters can be set individually for each cell type as well as between different cell types for inter-cell interactions. We only vary the growth-force strength G^{α} and adhesion strength $f_1^{\alpha\beta}$ between cells of the same ($\alpha = \beta$) and different ($\alpha \neq \beta$) cell types, respectively, where α and β are cell-type numbers. We report simulation parameters relative to a standard host cell type (see SI for numerical values, which is available online at stacks.iop.org/NJP/22/033048/mmedia), denoted with a dagger, e.g. $G^{\dagger} = G/G^0$. Time is measured in terms of the inverse apoptosis rate k_{a}, distance in units of the pair potential cut-off length R_{PP} and stresses in units of G^0/R_{PP}^4. Quantities reported in these units are denoted by an asterisk *. All simulations are performed in a cubic box with edge length $L = 12 \cdot R_{\mathrm{PP}}$ and periodic boundary conditions in all directions, unless stated otherwise.

Tumor cells even within the same tumor are not all identical, but vary in terms of all kind of attributes, e.g. expression levels of different proteins [42] or their reaction to certain treatments [43]. Hence, there is not only a competition between the tumor and the host, but also between cell-subpopulations of the tumor. Different models exist to describe tumor heterogeneity, e.g. cancer stem cells [44] or clonal evolution [45]. In the latter case, a tumor originates from a single mutated cell, which can acquire additional mutations over time, yielding additional subpopulations. We model this behaviour by defining a fixed number n of different 'genotypes', each having a different growth-force strength G^{α} and adhesion strength $f_1^{\alpha\alpha}$. Mutations are implemented by offering each daughter cell after a division event the chance to change its genotype with a certain probability. Cancer cells typically have much higher mutation rates than healthy cells, e.g. due to misfunction of the error correction machinery during DNA replication [6, 46, 47]. Even for a moderate mutation rate a cell can acquire many mutations over several generations [48]. However, how many of these mutations actually lead to phenotypic variations and changes of the mechanical properties of a cell remains an open question. We therefore study the influence of the mutation rate on our results systematically.

In tissues, several adhesion mechanisms exist, serving a variety of different functions to maintain tissue integrity. Between epithelial cells, the strength of cell–cell adhesion is to a large degree regulated by anchoring junctions, e.g. adherens junctions, which connect the actin cytoskeletons of neighbouring cells. Adherens junctions are mediated by cadherins, which form homophilic bonds between cells. Thus, the strength of adhesion between cells is limited by the cell expressing less cadherin, or, in terms of our simulation model $f_1^{\alpha\beta} = \min(f_1^{\alpha\alpha}, f_1^{\beta\beta})$. A reduced adhesion strength yields a higher homeostatic pressure [38], which is otherwise dominated by the growth-force strength G.

Naturally such a minimalistic model can not cover the full complexety of real tumor development. How random are mutations? How likely do these mutations alter the mechanical properties of a cell? What is the role of the biochemical microenvironment? Instead our model focuses on generic aspects of mechanics alone. The two key aspects underlying this work, the evolutionary nature of cancer and the observed mechanical alterations of cancer cells, are well established in the literature [1, 2, 49, 50]. Our aim is to study the combined action of these two aspects of cancer, while the complexity of real tumors will have to be integrated stepwise in future studies.

3. Results

For free parameter evolution, the tissue evolves to a strong-growing and low-adhesive genotype (see figure 1), as predicted by the homeostatic pressure approach [15]. However, E-cadherin also plays a role in signaling processes connected to cell growth, and thus a reduced expression might come at the cost of a lower growth-force strength G, which in turn yields a lower homeostatic pressure. We thus turn our attention to the case where an increase in growth-force strength G^{α} comes at the cost of a higher self-adhesion strength $f_1^{\alpha\alpha}$. We assume the relations as

$$G^{\alpha} = (1 + D^{\alpha})G^0 \tag{3}$$

$$f_1^{\alpha\alpha} = (1 + D^{\alpha} \cdot \tau)f_1^0, \tag{4}$$

with genotype number α in the range $[-(n-1)/2, (n-1)/2]$, evolutionary distance $D^{\alpha} = d \cdot \alpha$, distance d between neighbouring genotypes and tradeoff paramteter τ (with $G^{\alpha}, f_1^{\alpha\alpha} > 0 \ \forall \alpha$). After a division event, each daughter cell might mutate into a new genotype with probability p_{m}. If the cell mutates, its genotype number is changed to $\alpha_{\mathrm{mother}} \pm 1$ randomly. This yields a mutation rate $k_{\mathrm{m}} = 2p_{\mathrm{m}}k_{\mathrm{a}}$.

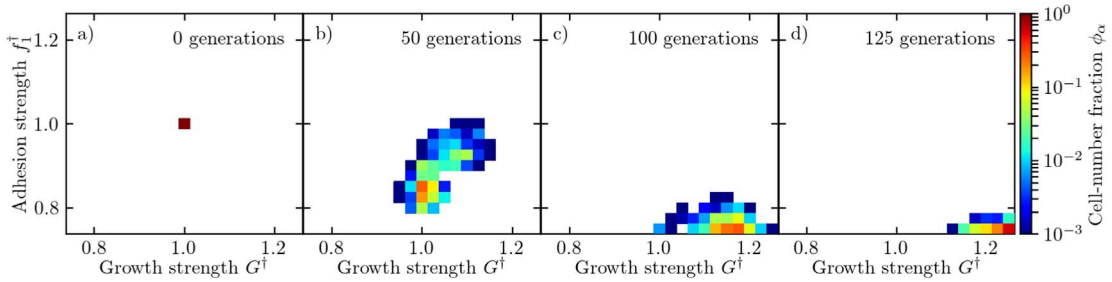

Figure 1. Evolution of a tissue with mutations altering growth-force strengh $G^\dagger$ and adhesion strength $f_1^\dagger$ independently. Heatmaps displaying cell-number fractions after (a) zero generations (initial condition), (b) 50 generations, (c) 100 generations and (d) 125 generations. See video S1 for a movie of the time evolution of the heatmap.

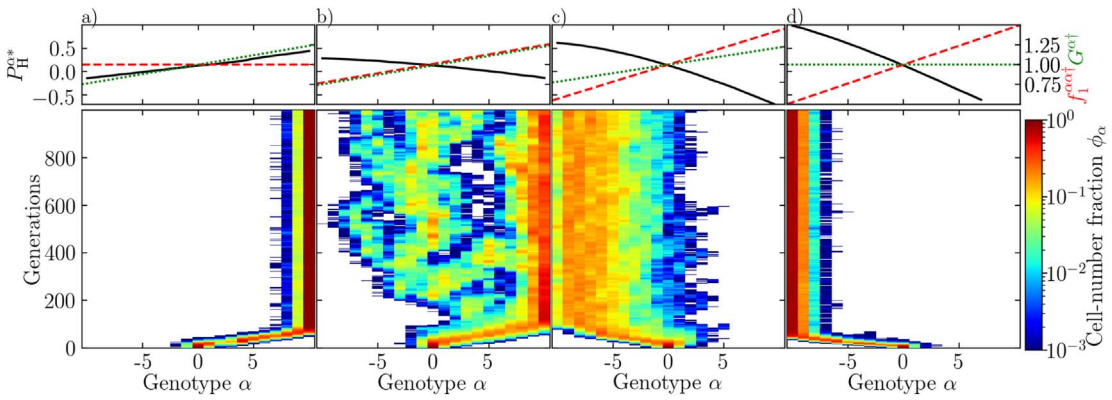

Figure 2. Time evolution of the genotype number fractions ϕ_α for tradeoff paramter (a) $\tau = 0$, (b) $\tau = 1$, (c) $\tau = 2$ and (d) $\tau \to \infty$, $d \to 0$. Simulations start from a host (standard) tissue at homeostasis, with $n = 21$ genotypes, $p_m = 0.01$ in all and $d = 0.025$ in (a)–(c). White space corresponds to times where no cells of the genotype exist. Color is coded on a logarithmic scale. Curves above display homeostatic pressure $P_H^{\alpha*}$ (black solid), growth-force strength $G^{\alpha\dagger}$(red dashed) and self adhesion strength $f_1^{\alpha\alpha\dagger}$ (green dotted) of the corresponding genotype number α. See video S2 for a visualization of the temporal evolution of a tissue with $\tau = 1.25$.

Figure 2 displays results of such simulations for four different cases: only variation of growth-force strength ($\tau = 0$), balanced tradeoff ($\tau = 1$), adhesion strength varied twice as much as growth-force strength ($\tau = 2$) and only variation of adhesion strength ($\tau \to \infty$). Without tradeoff (figure 2(a)), the tissue evolves towards the strongest growing genotype or, equivalently, the one with the highest homeostatic pressure. Similarly, for $\tau \to \infty$ (figure 2(d)), the system evolves towards the lowest adhesive genotype (again, the one with the highest P_H). We find the most dynamic evolution for a balanced tradeoff (figures 3 and 2(b)). At first, the system evolves to stronger growing and more adhesive genotypes. Over time a noticable fraction of cells evolves also towards weak-growing, less adhesive genotypes. The genotype number fractions $\phi_\alpha = N_\alpha/N$ (with individual and total number of cells, N_α and N), show large fluctuations (see figures 3(b) and (c)), with individual genotypes not being populated at all for certain time periods. Besides this highly dynamic temporal evolution, after an initial time period the system is dominated by genotypes with increased growth force and adhesion strength at all times, with the one at the upper boundary having the highest number fraction for most of the time (see figure 3(a)). This result comes at a surprise, as this is also the genotype with the lowest homeostatic pressure, while the one at the lower boundary, which is basically never populated, has the highest P_H. For a higher tradeoff (figure 2(c)), we still find a broad distribution of genotypes, with less adhesive genotypes dominating over the stronger growing ones, i.e. the loss in growth-force strength is overcompensated by a lower adhesion strength. Interestingly, these results are not altered qualitatively by additional randomness in the division mechanism or a reduced mutation propability (see SI).

In order to gain insight into the underlying mechanism of this dynamic evolution, we study the competition between two genotypes and no mutations ($p_m = 0$). Simulations are started from a single mutated cell (with increased/decreased growth force and adhesion strength) in a host tissue at the homeostatic state (we label the mutant with M and the host (wild type) with W). Even in this simplified case, we find one parameter regime in which the mutant is not able to grow, one regime with stable coexistence in a highly mixed state and another regime in which the mutant outcompetes the host. Figure 4 shows the averaged number fractions of the mutant

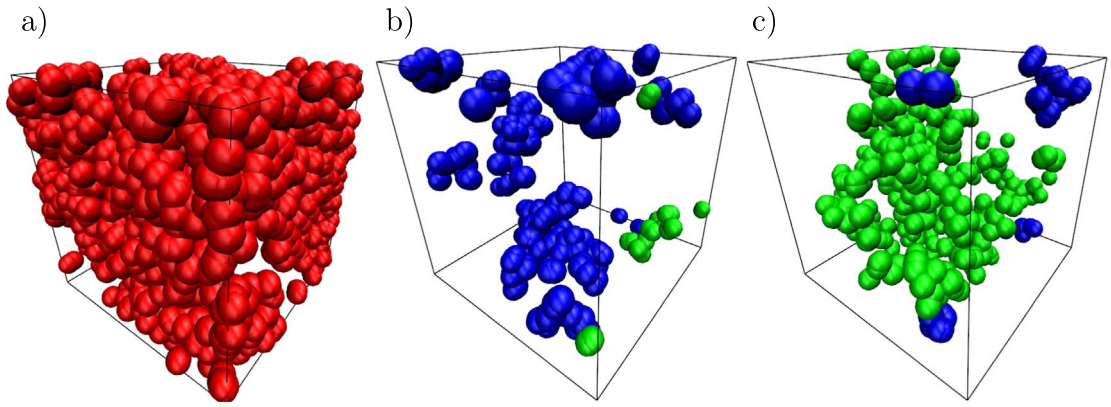

Figure 3. Simulation snapshots obtained from the simulation shown in figure 2(b). (a) The dominating genotype ($\phi_{10} = 0.283$) after 1000 generations. (b) Genotype $\alpha = -6$ (blue) and $\alpha = 6$ (green) after 485 generations ($\phi_{-6} = 0.027$, $\phi_6 = 0.002$). (c) Same as (b), but after 910 generations ($\phi_{-6} = 0.003$, $\phi_6 = 0.045$).

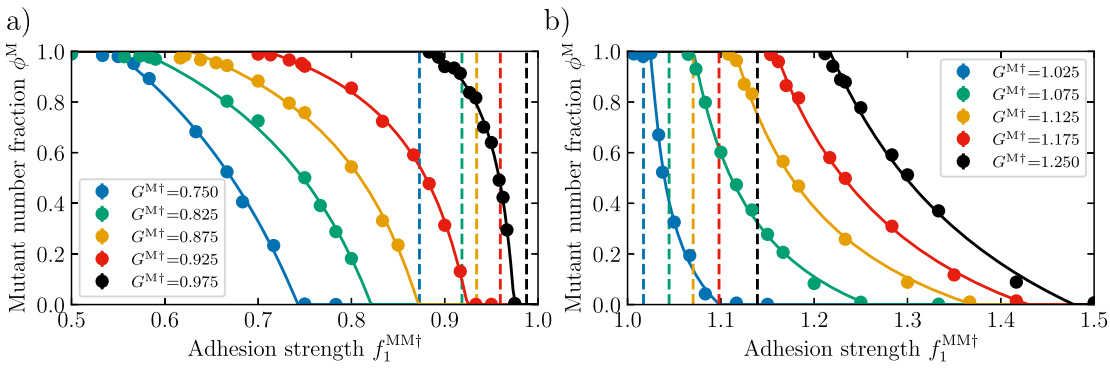

Figure 4. (a) Average number fraction ϕ^M of the mutant in terms of its adhesion strength $f_1^{MM\dagger}$ for various (reduced) growth-force strengths $G^{M\dagger}$. Error bars are obtained via block-averaging method (hidden behind markers) [51]. Dashed vertical lines indicate the points below which the mutant has a higher homeostatic pressure, solid lines are fits to equation (10). (b) Same as in (a) but for increased growth force and adhesion strengths of the mutant.

at the steady state. For reduced growth force and adhesion strength (figure 4(a)), the mutant can only grow against the host if its adhesion strength is reduced below a critical f_1^{crit}. In terms of equation (4), the value of f_1^{crit} roughly corresponds to a balanced tradeoff ($\tau \approx 1$). Already for $f_1^{MM} > f_1^{crit}$, the homeostatic pressure of the mutant exceeds the one of the host, i.e. a parameter regime exists in which the mutant is not able to grow, despite of the higher P_H. The reverse happens when growth force and adhesion strength are increased. The mutant completely takes over the compartment, although its homeostatic pressure is smaller than that of the host. Again, coexistence is only found when the adhesion strength is increased above f_1^{crit}. In the coexistence regime, the mutant number fraction scales as $\phi^M \propto 1/(f_1^{MM} - f_1^{WW})$.

Altogether, the competition between two genotypes alone yields the same qualitative results as the more complex multi-genotype case discussed before. Still, the question remains how a genotype with a lower homeostatic pressure can outcompete a genotype with a higher homeostatic pressure. The answer can only lie in the adhesion strength $f_1^{MW} = \min(f_1^{MM}, f_1^{WW})$ between mutant and host cells. This choice of cross-adhesion strength breaks symmetry, as the stronger adhering genotype has more free space at the interface, which favors divisions [19].

To address this question, we develop a phenomenological model which incorporates pressure-dependent growth as well as interfacial effects, in order to obtain a qualitative explanation of the simulation results.

We start with the expansion of the bulk growth rate k_b around the homeostatic pressure,

$$k_b = \kappa(P - P_H), \tag{5}$$

with the pressure response coefficient κ. Due to the high degree of mixing, the number fractions $\phi^{M/W}$ and hence the strengh of interfacial effects vary locally. In a mean-field approximation, we take the interfacial effects to be proportional to $\phi^M(1 - \phi^M)$, with individual prefactors $\Delta k_s^{M/W}$ for each genotype. The time evolution is then given by

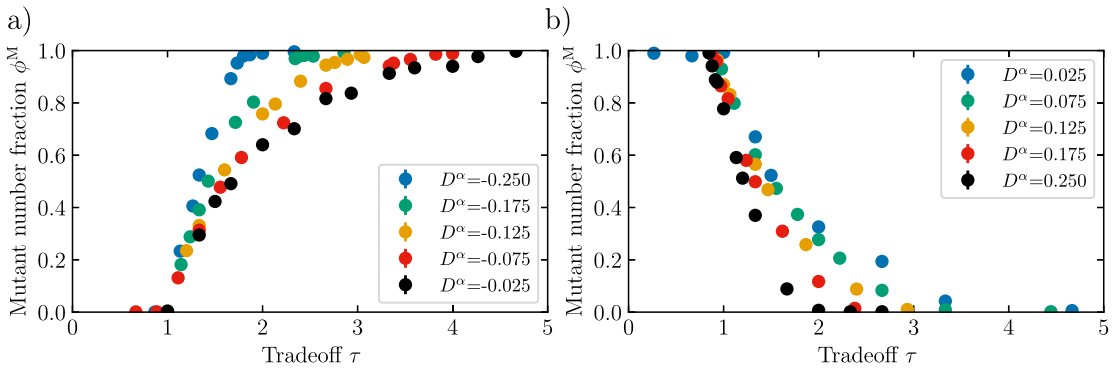

Figure 5. (a) Average number fractions of the mutant (same simulations as shown in figure 4(a)) as a function of the tradeoff τ of equation (4) for different evolutionary distances D^α. (b) Same as in (a) but with results from figure 4(b). Error bars are obtained via block-averaging method (hidden behind markers).

$$\partial_t \phi^M = \kappa(P_H^M - P)\phi^M + \Delta k_s^M \phi^M (1 - \phi^M) \tag{6}$$

$$\partial_t (1 - \phi^M) = \kappa(P_H^M + \Delta P_H - P)(1 - \phi) + \Delta k_s^W \phi^M (1 - \phi^M), \tag{7}$$

with the difference in homeostatic pressure $\Delta P_H = P_H^W - P_H^M$. Addition of equations (6) and (7) yields the pressure

$$P = P_H^W - \Delta P_H \phi^M + \frac{\Delta k_s^M + \Delta k_s^W}{\kappa} \phi^M (1 - \phi^M). \tag{8}$$

Thus, the pressure is given by the homeostatic pressures of the two genotypes weighted by their number fraction plus an interfacial term. A figure displaying the pressure measured during the simulations shown in figure 4 can be found in the SI. Insertion of equation (8) into (6) yields a differential equation for the number fraction with three fixed points ($\partial_t \phi^M = 0$), $\phi_1^M = 0$, $\phi_2^M = 1$, and

$$\phi_3^M = \frac{-\kappa \Delta P_H + \Delta k_s^M}{\Delta k_s^M + \Delta k_s^W}. \tag{9}$$

We discuss this result for the case of reduced growth force and adhesion strength of the mutant. Δk_s^M might be expected to vanish, as $f_1^{MM} = f_1^{MW}$ and mutant cells thus would not feel whether neighbouring cells are mutant or host cells. However, in order to grow, a cell needs to impose a strain on its surrounding. Host cells adhere more strongly to each other, thus it is harder for a mutant cell to impose a strain when surrounded by host cells. Hence, Δk_s^M is actually negative and the homeostatic pressure of the mutant needs to exceed the host pressure by $-\Delta k_s^M/\kappa$ in order to be able to grow against the host. At this point, ϕ_3^M becomes positive, as long as $\Delta k_s^M + \Delta k_s^W > 0$. Host cells can impose a strain more easily when surrounded by mutant cells and, additionally, have more free space than when surrounded by other host cells. Hence, $|\Delta k_s^M| < \Delta k_s^W$ and the above mentioned condition is fulfilled. Similarly, coexistence can be found for increased growth force and adhesion strength when $\Delta P_H > -\Delta k_s^W/\kappa$. The above mentioned scaling of the mutant number fraction can be obtained by an expansion of ΔP_H and $\Delta k_s^{M/W}$ to linear order in terms of $\epsilon := (f_1^{MM} - f_1^{WW})/f_1^{WW}$ in equation (9),

$$\phi_3^M = \frac{-\kappa \Delta P_H^0}{(\Delta k_s^{M1} + \Delta k_s^{W1})\epsilon} + \frac{-\kappa \Delta P_H^1 + \Delta k_s^{M1}}{\Delta k_s^{M1} + \Delta k_s^{W1}}. \tag{10}$$

The zeroth order terms of $\Delta k_s^{M/W}$ vanish as there are no interfacial effects when the adhesion strength between host and mutant cells is equal to their self-adhesion strength, while ΔP_H^0 can be non-zero due to a changed growth-force strength. Indeed, equation (10) reproduces the simulation data reasonably well (see figure 4). A discussion of the numerical values of the fitted parameters and additional results can be found in the SI.

Figure 5 displays similar results as shown in figure 4, but now as a function of the tradeoff τ in equation (4). For $\tau < 1$ the genotype with higher growth-force strength outcompetes the weaker genotype, for $1 < \tau < 2$ a transition towards the less adhesive genotype occurs, while for even higher values of the tradeoff $\tau > 2$ the less adhesive genotype outcompetes the second genotype. This transition from strongly growing, adhesive to weakly growing, less adhesive genotypes is found in the same range of τ as in the competition between many genotypes. Hence, the simplified case of two competing genotypes captures the essential physics to explain the coexistence between many competing genotypes and, additionally, provides a quantitative description.

Next, we turn our attention to the effect of a finite mutation rate on the evolution of the system. Figure 6(a) shows the number fraction of the mutant as a function of k_m for different combinations of evolutionary distance

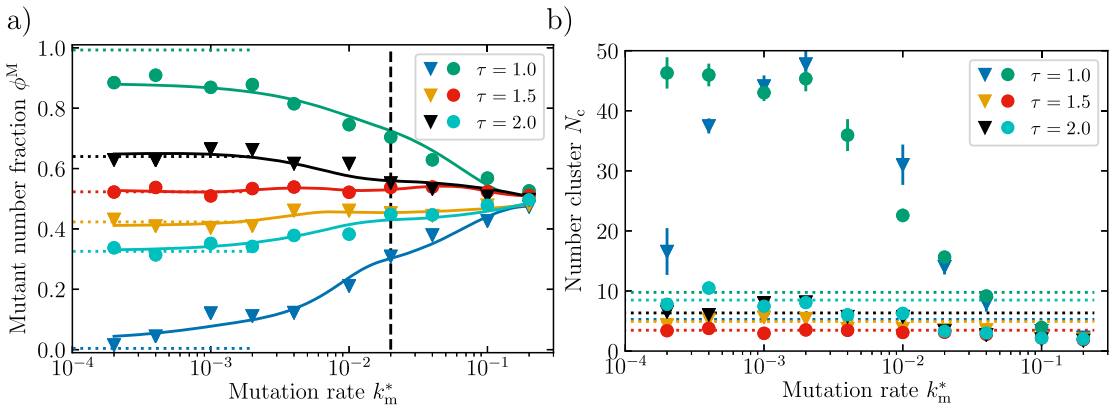

Figure 6. (a) Average number fraction ϕ^M of the mutant as a function of the mutation rate k_m^* for different values of the tradeoff τ, for evolutionary distances $D^\alpha = 0.025$ (circles) and $D^\alpha = -0.025$ (triangles). Horizontal dotted lines display results for a single mutation event. Vertical black dashed line indicates standard mutation rate. Solid lines are a guide to the eye. (b) Average number of clusters of the weaker genotype N_c measured in the same competitions in (a). Horizontal dotted lines display results for a single mutation event. Error bars are obtained via block-averaging method.

D^α and tradeoff τ, in comparision to the number fraction reached for a single mutation event. As expexted, the number fraction converges towards $1/2$ with increasing k_m for all combinations. For moderate mutation rates, however, the number fraction largely fluctuates around the same average as of a single mutation event. The single mutation leads to a stable coexistence of the two genotypes—additional mutations quickly relax back to this state. Significant deviations occur only if in the steady state of the single mutation event the number fraction of one genotype is close to zero (in the following termed the weaker genotype, while, vice versa, the genotype with number fraction close to one is termed the stronger genotype). In that case, the weaker genotype consists only of one or very few small cohesive clusters of cells, because cells of the weaker genotype need to detach from the primary cluster in order to form new clusters, but are likely to die when they do so, as they are only surrounded by cells of the stronger genotype. Hence, the distribution of cells is highly non-homogenous. Compared to the single mutation event, even a small mutation rate leads to the formation of multiple small cluster all over the system, thus increasing the number fraction of the weaker genotype (see figure 6(b)) for comparision in terms of number of clusters and SI for further discussion). This result explains why at least two genotypes, in addition to the dominating genotype, are populated as well in the cases shown in figures 2(a) and (d). When the number fractions of both genotypes are sufficiently large (for $1 \leqslant \tau \leqslant 2$), deviations from the average of a single mutation are still small for the standard mutation probability. Additionally, in the competitions between many genotypes, mutations change the genotype to $\alpha \pm 1$ randomly and not in a preferred direction. Hence, we conclude that the precise value of the mutation probability does not play an important role in the regime where we find a heterogeneous distribution of genotypes, as long as it is reasonably small ($k_m \ll k_a$).

Given that a single mutated cell can grow to tissue of macroscopic size in a certain parameter regime for $f_1^{MW} = \min(f_1^{MM}, f_1^{WW})$, the question arises how likely it is to actually reach this state. In order to study this probability, we mutate again a single cell in a host tissue at its homeostatic state. A mutation that reaches a certain threshold $N_t = 20$ of cells counts as a survival event (the chance to die after reaching this treshold becomes extremely small), apoptosis of the last mutant cell as a death event. Figure 7 shows the averages of many such simulations. For reduced growth force and adhesion strength, the survival probability p_s is only non-zero below the critical adhesion strength f_1^{crit}. For $f_1^{MM} < f_1^{crit}$, p_s increases linearly with further decreasing adhesion strength. On the other hand, when growth force and adhesion strength are increased, the survival probability first shows a plateau, whose value increases with increasing growth force strength, from which it will probably drop to zero with further increase. Simulations in this regime are difficult, because a mutated cell can easily grow to a few cells, but will hardly reach the number threshold nor completely vanish again. Due to the high self-adhesion strength on the one hand, it becomes hard to detach from the other cells, but on the other hand easy to grow against the host when only few or no other mutant cells are around. This explains the larger error bars at the highest values of the adhesion strength, where the sample size is small.

4. Discussion

We have shown how intra-tumor heterogeneity, the existence of multiple subpopulations within the same tumor, can arise due to mechanical interactions alone, while most studies on evolutionary dynamics in tumors

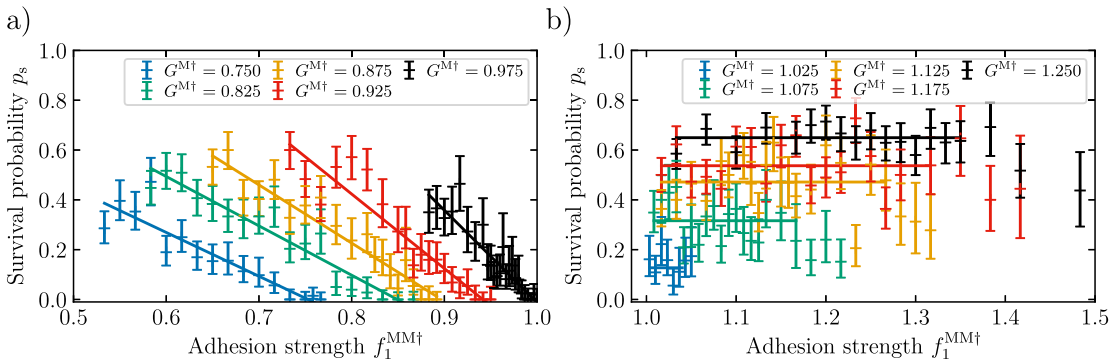

Figure 7. (a) Probability p_s of a single mutated cell to grow to macroscopic size as a function of its (reduced) adhesion strength $f_1^{\mathrm{MM}\dagger}$ for several values of the (reduced) growth-force strength $G^{\mathrm{M}\dagger}$. Error bars are a 1σ binomial confidence interval obtained by Clopper-Pearson. Solid lines are linear fits. (b) Same as in (a), but with a constant fitted in the plateau regime and increased growth force and adhesion strength. Box size $L^* = 8$.

focussed on the adaptation to chemotherapy and development of resistance to certain drugs [20, 21]. The simultaneous change of the adhesion and growth-force strength stabilizes the coexistence of multiple subpopulations, in a highly dynamic state. A higher growth-force strength alone, as well as a lower adhesion strength, favor proliferation of a single subpopulation and the evolution of the system to cell types with the highest growth-force strength, or lowest adhesion strength, respectively. A tradeoff between the two, however, yields coexistence between multiple subpopulations of different cell types. Interestingly, the expression of the adhesion protein E-cadherin, which also affects cell growth, has been found to be down-regulated in many real tumors [28].

The simulations also reveal that the homeostatic pressure of a cell type is not necessarily the only quantity that determines the result of a competition. Interactions between different cell types, in our model determined by the adhesion between them, can lead to a completely reverse outcome, i.e. a cell type with a lower homeostatic pressure can outcompete a cell type with a higher homeostatic pressure completely. A phenomenological model explains the results on a qualitative level. The evolution of each cell type is governed by mechanically-regulated growth, while mutation rates only play a minor role in the dynamics.

We have focussed here on tissue evolution driven by mechanics alone, neglecting other possible selection forces which determine the overall fitness of a subpopulation in a real tumor, which consequently affects its evolution. Possible examples are spatially varying distributions of growth-limiting resources or presence of chemotherapeutic drugs. This could be included into our simulation model by making certain model parameters, e.g. growth-force strength or apoptosis rate, dependent on the local concentration of these substances [52]. An interesting future aspect for competition regulated purely by mechanics is the influence of open boundaries. A tissue with a negative homeostatic pressure then naturally grows to a spheroid of finite size, with an enhanced rate of division at the surface [38]. For competing cell types, this would lead to an interplay between surface and interfacial effects.

Acknowledgments

The authors gratefully acknowledge the computing time granted through JARA-HPC on the supercomputer JURECA [53] at Forschungszentrum Jülich. Parts of the simulations were performed with computing resources granted by RWTH Aachen University under project rwth0475.

Data availability

The simulation code and data are made available in an open data repository under the DOI 10.5281/zenodo.347923.

ORCID iDs

Tobias Büscher https://orcid.org/0000-0002-5009-1479
Gerhard Gompper https://orcid.org/0000-0002-8904-0986
Jens Elgeti https://orcid.org/0000-0001-7300-0923

References

[1] Weinberg R A 2007 *The Biology of Cancer* (New York: Garland Science)
[2] Greaves M and Maley C C 2012 *Nature* **481** 306
[3] Bozic I *et al* 2013 *eLife* **2** e00747
[4] Vogelstein B and Kinzler K W 1993 *Trends Genet.* **9** 138–41
[5] Heppner G H 1984 *Cancer Res.* **44** 2259–65 http://cancerres.aacrjournals.org/content/44/6/2259
[6] Preston B D, Albertson T M and Herr A J 2010 *Semin. Cancer Biol.* **20** 281–93
[7] Schnekenburger M and Diederich M 2012 *Curr. Colorectal Cancer Rep.* **8** 66–81
[8] Petrova Y I, Schecterson L and Gumbiner B M 2016 *Mol. Biol. Cell* **27** 3233–44
[9] Padmanaban V, Krol I, Suhail Y, Szczerba B M, Aceto N, Bader J S and Ewald A J 2019 *Nature* **573** 439–44
[10] Wernig F and Xu Q 2002 *Prog. Biophys. Mol. Biol.* **78** 105–37
[11] Cheng G, Tse J, Jain R K and Munn L L 2009 *PLoS One* **4** e4632
[12] Montel F *et al* 2011 *Phys. Rev. Lett.* **107** 188102
[13] Alessandri K *et al* 2013 *Proc. Natl Acad. Sci. USA* **110** 14843–8
[14] Helmlinger G, Netti P A, Lichtenbeld H C, Melder R J and Jain R K 1997 *Nat. Biotechnol.* **15** 778–83
[15] Basan M, Risler T, Joanny J F, Sastre-Garau X and Prost J 2009 *HFSP J.* **3** 265–72
[16] Williamson J J and Salbreux G 2018 *Phys. Rev. Lett.* **121** 238102
[17] Ranft J, Aliee M, Prost J, Jülicher F and Joanny J F 2014 *New J. Phys.* **16** 035002
[18] Podewitz N, Jülicher F, Gompper G and Elgeti J 2016 *New J. Phys.* **18** 083020
[19] Ganai N, Büscher T, Gompper G and Elgeti J 2019 *New J. Phys.* **21** 063017
[20] Burrell R A and Swanton C 2014 *Mol. Oncol.* **8** 1095–111
[21] Cunningham J J, Gatenby R A and Brown J S 2011 *Mol. Pharm.* **8** 2094–100
[22] Gallaher J A, Enriquez-Navas P M, Luddy K A, Gatenby R A and Anderson A R 2018 *Cancer Res.* **78** 2127–39
[23] Gatenby R A, Silva A S, Gillies R J and Frieden B R 2009 *Cancer Res.* **69** 4894–903
[24] Silva A S, Kam Y, Khin Z P, Minton S E, Gillies R J and Gatenby R A 2012 *Cancer Res.* **72** 6362–70
[25] Ghosh P, Mondal J, Ben-Jacob E and Levine H 2015 *Proc. Natl Acad. Sci. USA* **112** E2166–73
[26] Farrell F D, Gralka M, Hallatschek O and Waclaw B 2017 *J. R. Soc. Interface* **14** 20170073
[27] Jeckel H, Jelli E, Hartmann R, Singh P K, Mok R, Totz J F, Vidakovic L, Eckhardt B, Dunkel J and Drescher K 2019 *Proc. Natl Acad. Sci. USA* **116** 1489–94
[28] Beavon I 2000 *Eur. J. Cancer* **36** 1607–20
[29] Pece S and Gutkind J S 2000 *J. Biol. Chem.* **275** 41227–33
[30] Van Liedekerke P, Palm M M, Jagiella N and Drasdo D 2015 *Comput. Part. Mech.* **2** 401–44
[31] Farhadifar R, Röper J C, Aigouy B, Eaton S and Jülicher F 2007 *Curr. Biol.* **17** 2095–104
[32] Alt S, Ganguly P and Salbreux G 2017 *Phil. Trans. R. Soc.* B **372** 20150520
[33] Drasdo D and Höhme S 2005 *Phys. Biol.* **2** 133–47
[34] Schaller G and Meyer-Hermann M 2005 *Phys. Rev.* E **71** 051910
[35] Graner F and Glazier J A 1992 *Phys. Rev. Lett.* **69** 2013–6
[36] Szabó A and Merks R M 2013 *Front. Oncol.* **3** 87
[37] Basan M, Prost J, Joanny J F and Elgeti J 2011 *Phys. Biol.* **8** 026014
[38] Podewitz N, Delarue M and Elgeti J 2015 *EPL* **109** 58005
[39] Uroz M, Wistorf S, Serra-Picamal X, Conte V, Sales-Pardo M, Roca-Cusachs P, Guimerà R and Trepat X 2018 *Nat. Cell Biol.* **20** 646
[40] Basan M, Elgeti J, Hannezo E, Rappel W J and Levine H 2013 *Proc. Natl Acad. Sci. USA* **110** 2452–9
[41] Marel A K, Podewitz N, Zorn M, Rädler J O and Elgeti J 2014 *New J. Phys.* **16** 115005
[42] Marusyk A, Almendro V and Polyak K 2012 *Nat. Rev. Cancer* **12** 323–34
[43] Marusyk A and Polyak K 2010 *Biochim. Biophys. Acta* **1805** 105–17
[44] Shackleton M, Quintana E, Fearon E R and Morrison S J 2009 *Cell* **138** 822–9
[45] Nowell P 1976 *Science* **194** 23–8
[46] Hao D, Wang L and Di L J 2016 *Sci. Rep.* **6** 19458
[47] Bielas J H, Loeb K R, Rubin B P, True L D and Loeb L A 2006 *Proc. Natl Acad. Sci. USA* **103** 18238–42
[48] Tomlinson I P, Novelli M and Bodmer W 1996 *Proc. Natl Acad. Sci. USA* **93** 14800–3
[49] Katira P, Bonnecaze R T and Zaman M H 2013 *Front. Oncol.* **3** 145
[50] Remmerbach T W, Wottawah F, Dietrich J, Lincoln B, Wittekind C and Guck J 2009 *Cancer Res.* **69** 1728–32
[51] Allen M P and Tildesley D J 1989 *Computer Simulation of Liquids* (Oxford: Clarendon Press)
[52] Hornung R, Grünberger A, Westerwalbesloh C, Kohlheyer D, Gompper G and Elgeti J 2018 *J. R. Soc. Interface* **15** 20170713
[53] Jülich Supercomputing Centre 2018 *J. Large-Scale Res. Facil.* **4** A132